CLICdp-Conf-2018-012
21 December 2018

News on physics and detectors at CLIC

E. Brondolin*

On behalf of the CLICdp Collaboration

* *CERN, Switzerland*

Abstract

The Compact Linear Collider (CLIC) is a proposed high-luminosity linear electron-positron collider at the energy frontier. To optimise its physics potential, CLIC is foreseen to be built and operated in three stages, with a centre-of-mass energy from a few hundred GeV up to 3 TeV. In the first stage, CLIC will focus on the Higgs-boson and the top-quark properties, such as a high precision measurement of the Higgs total decay width and couplings and of the top-quark mass. During the subsequent energy stages, the aim of the physics programme will revolve around measurements of rare Higgs-boson processes, as well as direct and indirect searches for new physics, and precision measurements of possible new particles. To pursue this rich physics programme and to face the challenges imposed by the CLIC conditions, an optimised detector design and innovative new technologies are required. In this document, an overview of the CLIC accelerator, the CLICdet detector and its performance, and the CLIC physics programme is given.

Talk presented at New Trends in High-Energy Physics, Budva, Montenegro, 24–30 September 2018

1 Introduction

The Compact Linear Collider (CLIC) [1–3] is a mature options for a future high-luminosity linear electron-positron collider at the energy frontier. It is foreseen to be implemented in several energy stages with increasing centre-of-mass energy with the aim of measuring with high precision the properties of the top quark and the Higgs boson and searching for physics beyond the Standard Model (BSM). A recent update on the CLIC staging baseline scenario can be found in [4], where the assumptions about the accelerator ramp-up and up-time have been harmonised with those of other potential future colliders. In this new staging scenario CLIC is foreseen to run at the centre-of-mass energy of 380 GeV, 1.5 TeV and 3 TeV, and to deliver a total integrated luminosity of 1 ab^{-1}, 2.5 ab^{-1} and 5 ab^{-1}, respectively. The total integrated luminosity at 380 GeV CLIC stage includes about 100 fb^{-1} taken in an energy scan around the $t\bar{t}$ production threshold at 350 GeV. The CLIC baseline foresees also $\pm 80\%$ electron polarisation, and no positron polarisation. The luminosity per year and the total integrated luminosity in the updated scenario can be found in Figure 1.

2 CLIC accelerator

The high centre-of-mass energy of CLIC requires an accelerating gradient of 100 MV/m, using normal-conducting accelerating structure operating at 12 GHz. The CLIC accelerator features a novel acceleration scheme. In this technique, the deceleration of a high intensity beam, the so-called drive beam, in power-extraction and -transfer radio-frequency (RF) structures, is used to generate power in the RF cavities that accelerate particles of the colliding electron/positron beams, also called the main beam. The two-beam technique was demonstrated at CERN in the CTF3 test facility [2].

CLIC achieves high luminosities by using extremely small beam sizes, of the order of $(\sigma_x\ ,\ \sigma_y) = (40\,\text{nm},\ 1\,\text{nm})$. The beamstrahlung radiation emitted by the electron and positron bunches traversing the high field of the opposite beam produces two main types of background, incoherent e^+e^- pairs and $\gamma\gamma \rightarrow$ hadron events. While the former impacts mostly the particle occupancy in the detector and is mainly concentrated in the forward region, the latter has a more significant impact on the physics measurement due to the high energy deposits left in the detector. The effect of the beamstrahlung on the occupancy and the collision energy strongly depends on the centre-of-mass energy of CLIC as can be seen in Figure 2 and in Figure 3, respectively [5].

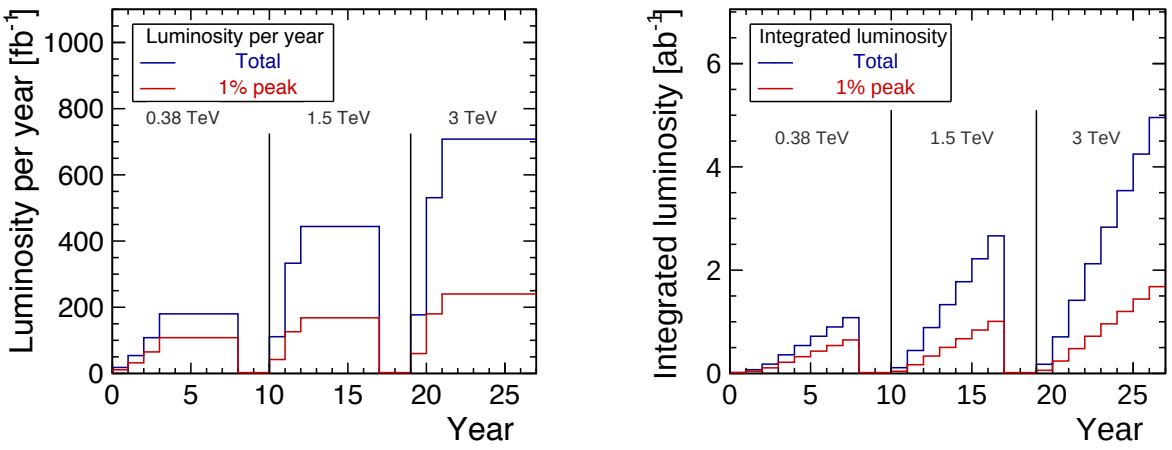

Figure 1: Luminosity per year (left) and the total integrated luminosity (right) in the updated CLIC scenario [4].

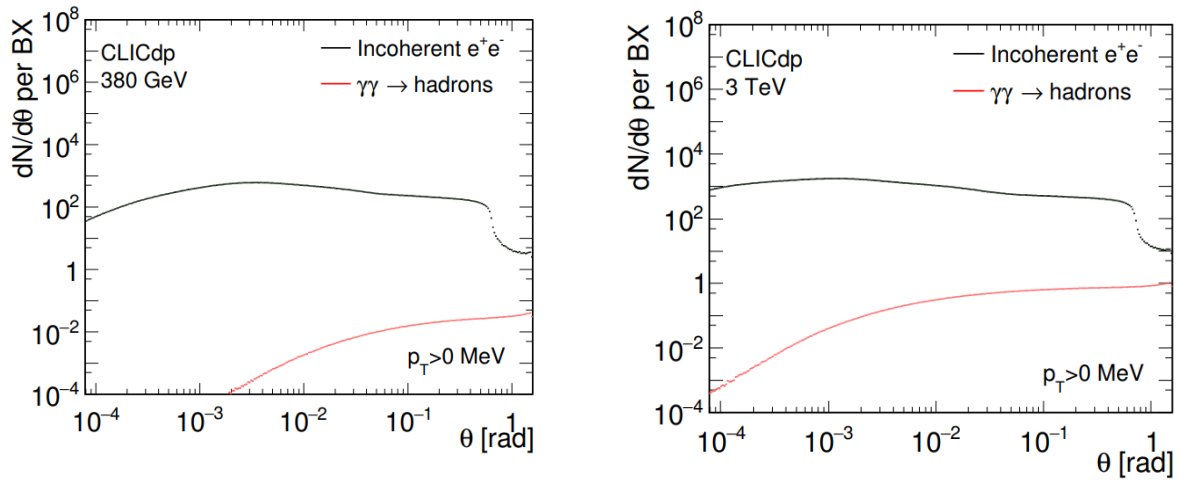

Figure 2: Angular distribution of the produced background particles in the case of 380 GeV (left) and 3 TeV (right) stage of the CLIC accelerator [5].

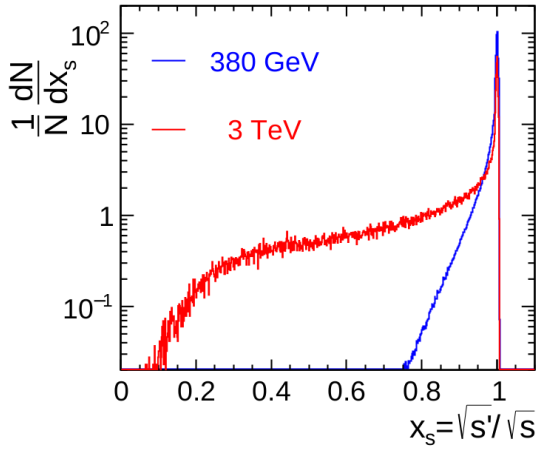

Figure 3: Luminosity spectrum at 380 GeV and 3 TeV stage of the CLIC accelerator [5].

Bunch trains of 312 (352) bunches at the 3 TeV (380 GeV) energy stage separated by 20 ms and single bunch separation of 0.5 ns in each bunch train allow for power pulsing in the detector and a trigger-less readout. To obtain excellent physics performance in trigger-less readout mode and to cope with the $\gamma\gamma \rightarrow$ hadron background, the subdetectors must provide a precise hit timing information which is used in offline software reconstruction as described in Section 3.1.

3 The detector for CLIC

CLICdet is a detector model designed to exploit the physics potential of the CLIC accelerator [6]. It foresees cutting-edge technology and is designed to obtain high performance using the Particle Flow Analysis (PFA). Moreover, it is optimised for the challenging conditions at CLIC, such as the bunches time structure and the high intensity $\gamma\gamma \rightarrow$ hadron background.

3.1 Detector requirements and optimisation

Some of the main detector requirements are the following:

- excellent track-momentum resolution for high-momentum tracks in the barrel, at the level of $\sigma_{p_T}/p_T^2 \leq 2 \times 10^{-5}\,\text{GeV}^{-1}$;
- precise impact-parameter resolution, at the level of $\sigma_{d_0}^2 = (5\,\mu\text{m})^2 + (15\,\mu\text{m}\,\text{GeV})^2/(p^2 \sin^3\theta)$, to allow accurate reconstruction and enable flavour tagging with clean b-, c-, and light-quark jet separation;
- jet-energy resolution for light-quark jets of $\sigma_E/E \leq 3.5\%$ for jet energies in the range 100 GeV to 1 TeV ($\leq 5\%$ at 50 GeV);
- detector coverage for electrons and photons to very low polar angles ($\sim$10 mrad) to assist with background rejection.

In order to fulfil these requirement, CLICdet features an ultra-low mass silicon tracking system, highly granular calorimeters, and subdetectors with a precise hit-timing resolution. The CLICdet layout follows the typical collider detector scheme. In the innermost part are placed a vertex detector composed of 25×25 μm^2 pitched pixels arranged in double-layers and a large tracker volume with barrel and disks of silicon micro-strips. The former is an extremely accurate subdetector with a single point resolution of 3 μm. All silicon tracking elements have a single hit time resolution of about $10/\sqrt{12}$ ns. The total tracker volume has a radius of 1.5 m and a half-length of 2.2 m with a total material budget less than $10\%X_0$ in the barrel region. Surrounding the tracker, an electromagnetic and hadronic calorimeter are placed, all embedded inside a superconducting solenoid providing a 4 T field. The basic ECAL structure of the CLIC detector is a silicon-tungsten sampling calorimeter with 5×5 mm^2 silicon detector cells, while the proposed hadronic calorimeter consists of steel absorber plates interleaved with 3×3 cm^2 scintillator tiles. The hit time resolution for all calorimeter hits is 1 ns. The outermost part of the detector is an iron yoke, interleaved with muon chambers. A quarter-view of CLICdet is shown in Figure 4. In the most forward part of CLICdet are placed two smaller electromagnetic calorimeters are placed, both built with layers of tungsten plates interleaved with sensors: LumiCal, covering an angular range from 39 mrad to 134 mrad, and BeamCal, covering from 10 mrad to 46 mrad.

The CLICdet geometry is optimised using a dedicated software suite which uses the DD4HEP software framework [7] and GEANT4 [8] via the DDG4 [9] package of DD4HEP for the geometry description and simulation. The design of the CLICdet concept ensures that the detector performance meets the requirements, as demonstrated in full simulation. An example of an event fully reconstructed with CLICdet and of an optimisation study aimed at establishing the outer tracker size taking into account the magnetic field and the p_T resolution goal is shown in Figure 5.

In full simulation, several studies were performed on the rejection of the beam-induced background from $\gamma\gamma \to$ hadrons. The energy deposit of these hadrons at the 3 TeV stage is around 20 TeV of energy per bunch train in the central calorimeters and as a consequence, their rejection is imperative to keep high physics performance. This can be efficiently done using the timing information coming from the subdetectors combined with additional p_T information on individually reconstructed particles. Figure 6 show the effectiveness of this selection for a typical $e^+e^- \to t\bar{t}$ event at centre-of-mass energies of 3 TeV [1, 10].

3.2 Detector performance

The CLICdet model fully satisfies the requirements described in Section 3.1. A detailed report on the CLICdet performance can be found in [5]. Some of the main results are summarised here.

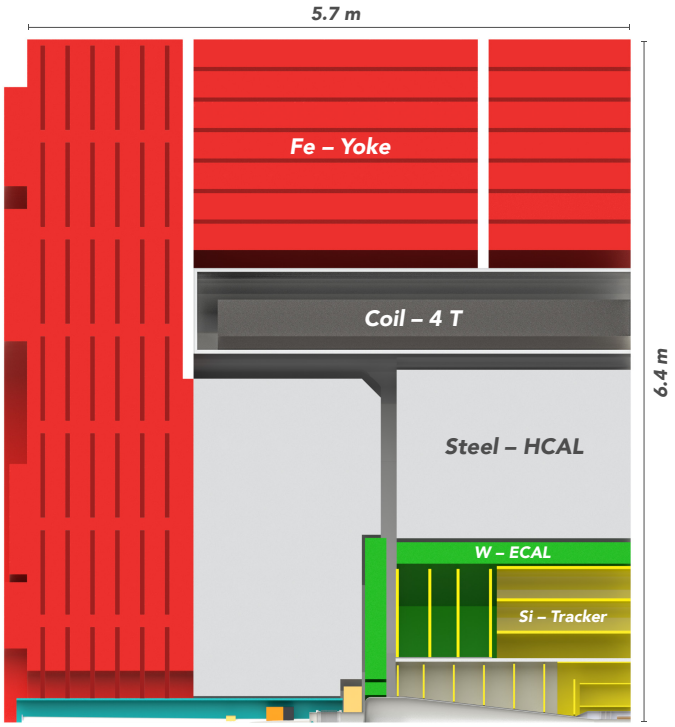

Figure 4: Longitudinal cross section of CLICdet [5].

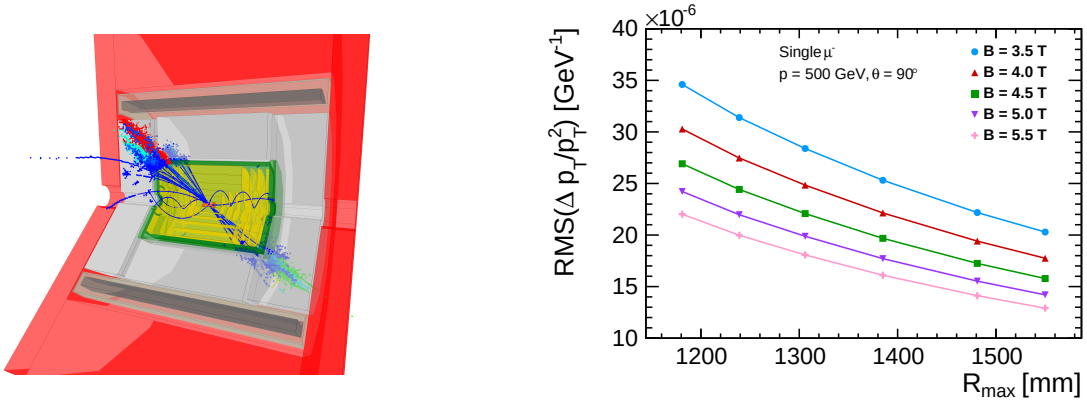

Figure 5: Event displays of $e^+e^- \to t\bar{t}$ events at a centre-of-mass energy of 3 TeV (left). Transverse momentum resolution as a function of tracker radius for different strengths of the B-field (right) [6].

Firstly, some highlights on the tracking performance can be found in Figure 7. On the left, the robustness of the conformal tracking algorithm used at CLICdet is shown in terms of tracking efficiency as a function of p_T for $e^+e^- \to t\bar{t}$ events with and without the $\gamma\gamma \to$ hadron events at the 3 TeV CLIC stage. In Figure 7 (right), the transverse momentum resolution for single muons as a function of the momentum in the case of different polar angles shows that the requirement on the resolution is achieved for high p_T tracks in the barrel.

Moreover, the choice of highly granular calorimeters and the optimisation of CLICdet to make full use of the PFA result in a very accurate jet energy resolution as shown in Figure 8 (left). Di-jet events using

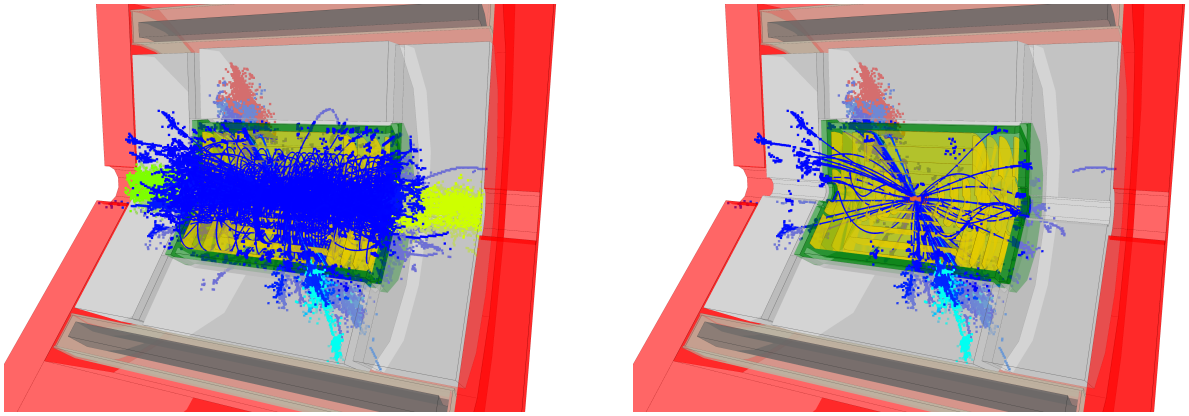

Figure 6: Event displays of $e^+e^- \to t\bar{t}$ events at a centre-of-mass energy of 3 TeV before (left) and after (right) background suppression using a timing selection.

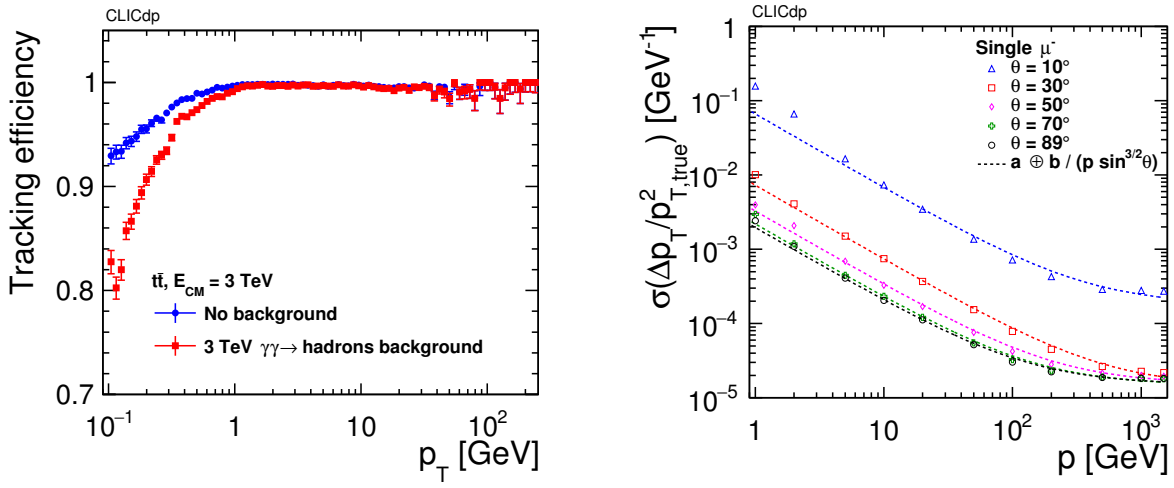

Figure 7: Tracking efficiency for $t\bar{t}$ events at the 3 TeV CLIC stage as a function of p_T with and without 3 TeV $\gamma\gamma \to$ hadron background overlay (left) and transverse momentum resolution for single muons produced at different polar angles as a function of the momentum (right) [5].

decays of a Z/γ^* particle into light quarks (u, d, s) at different centre-of-mass energies are analysed and the energy resolution for light-quark jets is found to be around $3-5\%$ for all jet energies with $|\cos\theta| < 0.925$, where θ is the quark polar angle. In Figure 8 (right) the efficiency for the electron reconstruction in the LumiCal as a function of the polar angle is shown in the case of the 3 TeV CLIC stage. Electrons with energy between 1.5 TeV and 190 GeV are reconstructed in the forward region with an efficiency well above 90% for all polar angles within the fiducial volume of LumiCal.

Finally, the performances of b- and c-flavour tagging at CLICdet are presented in Figure 9. In both cases the tagging results are shown using di-jet samples at 500 GeV without and with overlay of $\gamma\gamma \to$ hadron background produced at 3 TeV CLIC stage. On the left, the beauty quark misidentification probability is plotted as a function of the correct identification efficiency separately for charm and light-flavour contamination. In the right plot, the charm misidentification probability is assessed for beauty and light-flavour contamination. In both cases, the robustness of the flavor jet reconstruction and tagging is proven given that the effect of the background is only increasing the misidentification by a few percent.

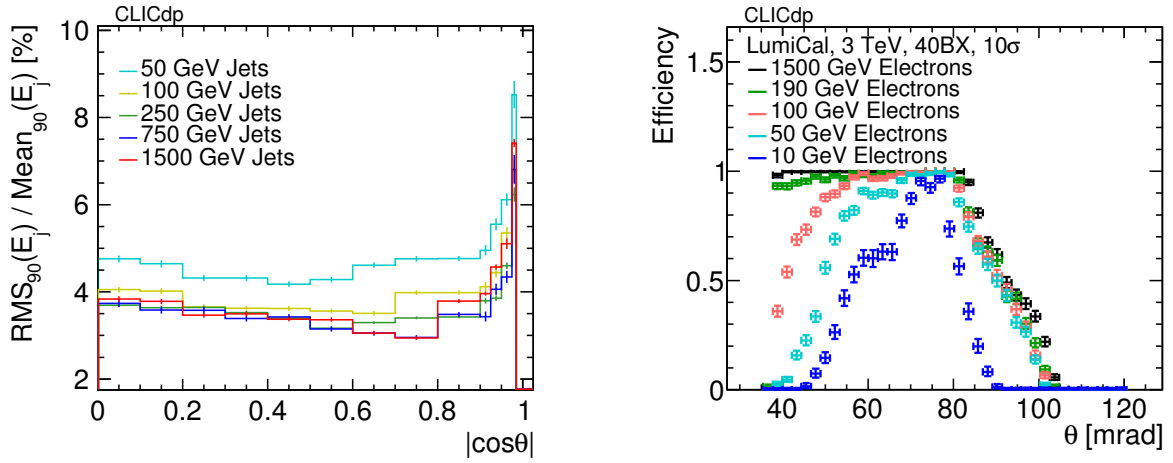

Figure 8: Energy resolution for light-quark jets as a function of the quark polar angle (left). Electron efficiency reconstruction in the LumiCal as a function of the polar angle at the 3 TeV CLIC stage (right) [5].

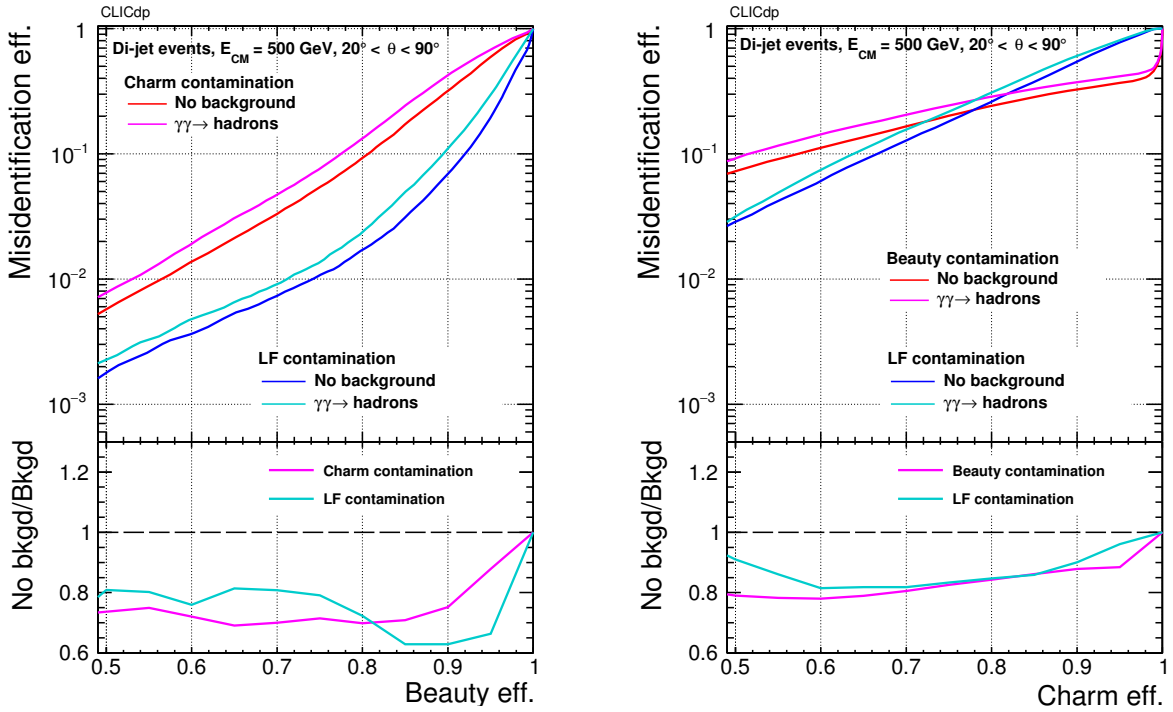

Figure 9: B-tagging (left) and c-tagging (right) performance for di-jet samples at 500 GeV without and with overlay of $\gamma\gamma \rightarrow$ hadron background produced at the 3 TeV CLIC stage [5].

4 Physics potential

CLIC, as a lepton collider with a wide range of energies and high luminosity, can pursue a physics programme with an unprecedented precision on many measurements in the Higgs and top-quark sector as well as potentially addressing several open questions exploring BSM physics.

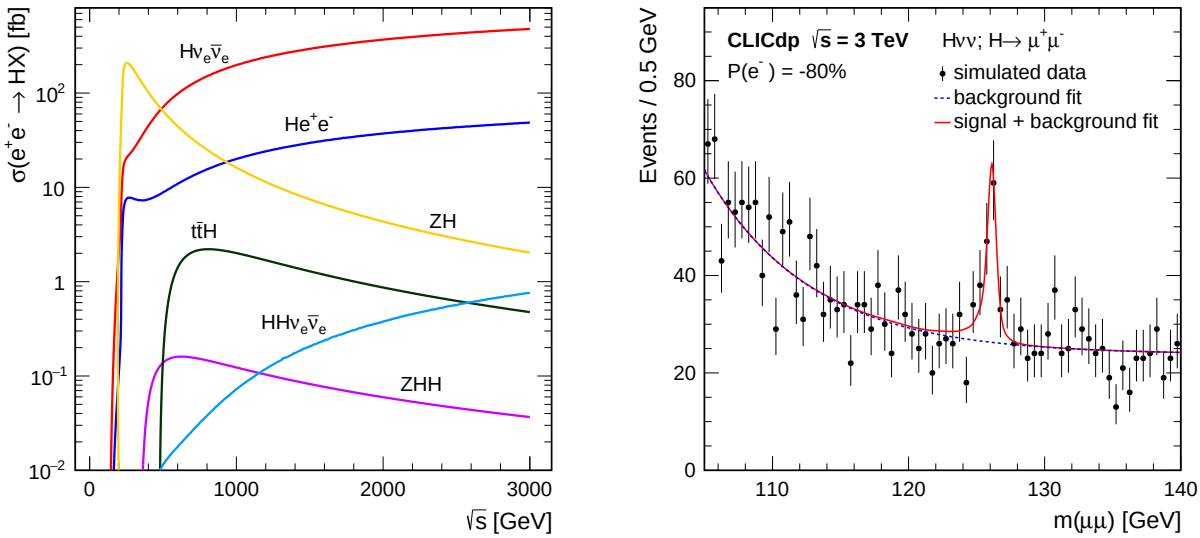

Figure 10: Higgs production cross sections for several production channels as a function of the centre-of-mass energy of an electron-positron collider (left) [1]. Reconstructed di-muon invariant mass distribution of selected $H \to \mu\mu$ events at the 3 TeV energy stage (right) [11].

4.1 Higgs physics

Studying the Higgs boson in great detail is one of the top priorities of the CLIC physics programme. The CLIC accelerator will produce and be able to reconstruct around 160 000 Higgs bosons during its initial stage, and millions are estimated for the highest energy stage. A detailed and comprehensive report on this topic can be found in [11], and including the latest update on the luminosity scenario in [4].

As shown in Figure 10 (left), the different energy stages of CLIC allow the study of several Higgs production channels as predicted in the Standard Model (SM). In the first CLIC stage, the Higgsstrahlung process $e^+e^- \to HZ$ is dominant. The Higgs boson can be identified event-by-event using only the Z boson recoil mass which allows for a measurement of the Higgs branching ratios and decay width without any assumptions about invisible BSM decays of the Higgs boson. At higher energy stages, the contribution from the WW-fusion process $e^+e^- \to H\nu_e\bar{\nu}_e$ becomes significant and can be used to improve the Higgs measurement precision. Moreover, rare processes become available such as the direct double-Higgs production $e^+e^- \to HH\nu_e\bar{\nu}_e$ which allows for the extraction of the trilinear Higgs self-coupling as well as the quartic HHWW coupling. In this study the possibility of polarising the electron beam plays an important role: the negative polarisation of -80% leads to an increase of the double-Higgs production cross section by a factor 1.8, while the positive polarisation of +80% reduces it by a factor of 0.2. The trilinear Higgs self-coupling can be determined at CLIC with a relative uncertainty of -7% and $+11\%$ at 68% C.L. under the SM parameters assumption.

As an example, the $H \to \mu^+\mu^-$ invariant mass distribution is shown in Figure 10 (right). Thanks to the high momentum resolution achieved by the CLIC detector, the peak is well visible on top of the background despite the very low SM branching ratio of 2×10^{-4}. In Figure 11, two results on the Higgs couplings and width are presented. On the left, the results obtained using a model-independent global fit are shown. Sub-percent precision can be obtained for the Higgs couplings (around 1% for rare decays), while the Higgs width can be extracted with precision of 2.5%. On the right, results for a model-dependent fit allow to compare CLIC with HL-LHC projection. It can be noted that, for several couplings, the precision achieved already at the first CLIC stage is significantly better than what is expected at HL-LHC.

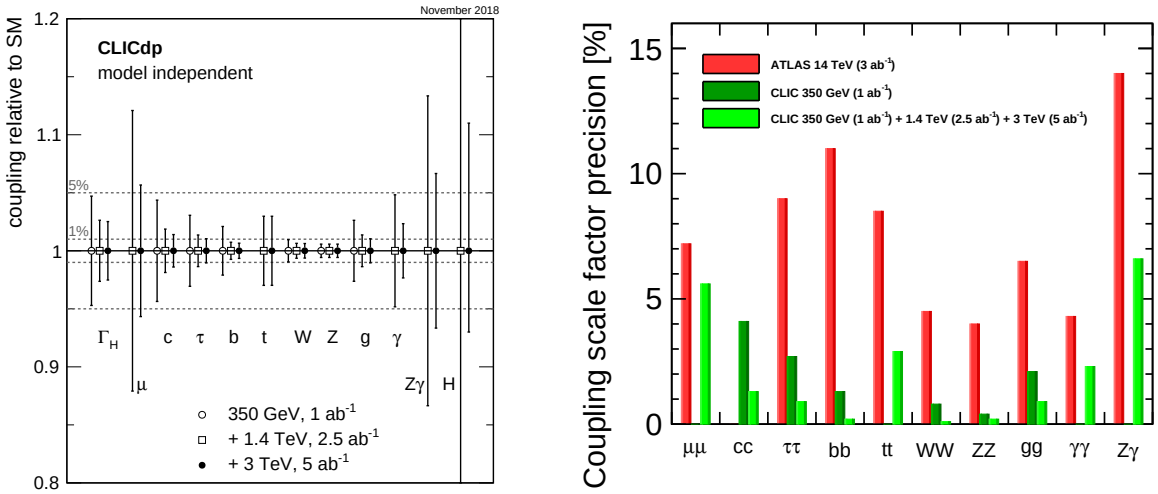

Figure 11: Precision on the Higgs couplings and width extracted from a model-independent global fit (left) [4]. Comparison between model-dependent Higgs coupling sensitivities measured at CLIC and corresponding HL-LHC projections (right) [4].

4.2 Top physics

Until now, the top quark has been produced only at hadron colliders. Therefore, CLIC would provide a unique opportunity to study this particle in detail, testing the SM limits and searching for possible BSM effects [12]. Depending on the energy stage, different aspects of top-quark production and properties can be studied.

In the first stage, CLIC foresees an energy scan around the top-quark pair-production threshold where samples of about $10\,\text{fb}^{-1}$ are recorded, separated by 1 GeV in collision energy as shown in Figure 12 (left). From the cross sections measured at each energy point, the top-quark mass, width and other model parameters are extracted using a template fit. The total uncertainty of the measurement on the top-quark mass amounts to about 50 MeV, mainly dominated by the present theoretical uncertainty. Moreover, $\text{t}\bar{\text{t}}$ events allow to search for top-quark decay modes produced by flavour-changing neutral-current processes which are strongly suppressed in the SM.

The higher energy stages of CLIC open the possibility of studying with high precision the top Yukawa coupling and CP properties in the ttH coupling. As an example, in Figure 12 (right) the sensitivity of the top-quark coupling to Z and γ in terms of form factors is reported [13]. The uncertainty on this measurement is particularly important to search for the existence of new heavy particles predicted by CP-violating new physics models which could modify the top-quark form factors. Already at the first stage, CLIC is able to perform a significantly more precise measurement than the HL-LHC. Finally, thanks to its highest centre-of-mass energy, CLIC is also the only currently proposed accelerator for which the vector boson fusion production process of top pairs $\text{e}^+\text{e}^- \to \text{t}\bar{\text{t}}\nu_\text{e}\bar{\nu}_\text{e}$ is accessible.

4.3 BSM physics

An extensive report on the CLIC potential for new physics was recently published [14]. Given that the relative BSM contribution in many models is expected to increase with centre-of-mass energy, CLIC operating at the highest energy stage provides significant discovery potential for BSM physics. BSM searches can be pursued through direct and indirect measurements.

Direct searches at the highest energy stage of CLIC have the potential to find new particles up to about 1.5 TeV with a 1% accuracy on their mass measurement. Their observation is easier in comparison

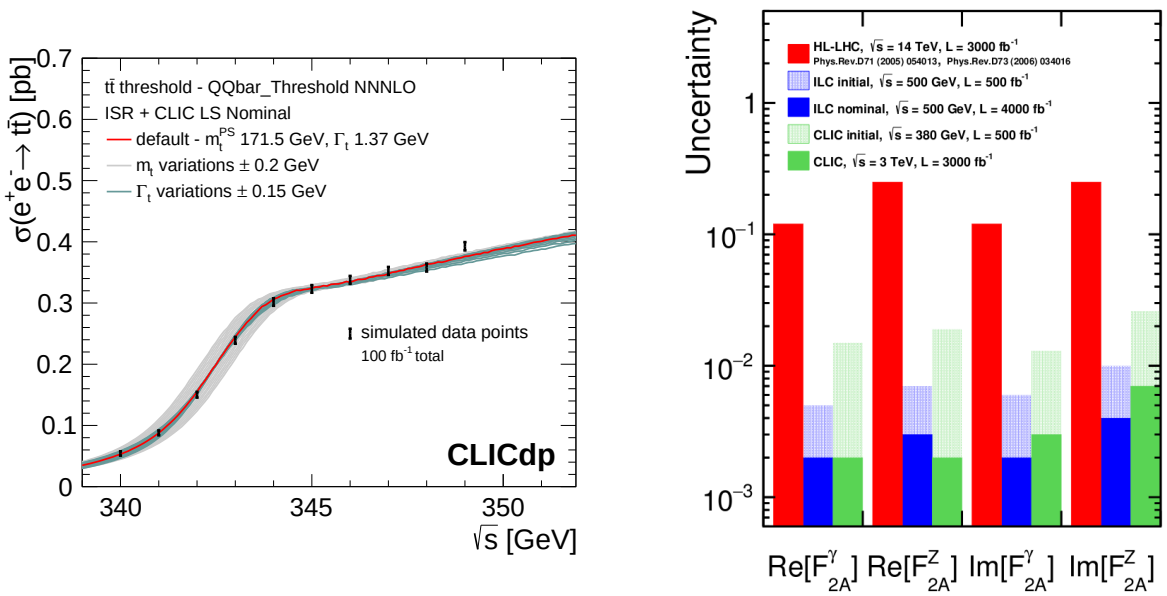

Figure 12: Top-quark threshold scan at CLIC with a total integrated luminosity of $100\,\mathrm{fb}^{-1}$ (left) [12]. Comparison of 68% C.L. limits on CP-violating form factors expected at the LHC, ILC and CLIC (right) [13].

to searches at hadron colliders thanks to the low background, and precision measurements of the new particle can also be performed after discovery. Such precise studies could also be conducted on new piarticles discovered at the LHC or the HL-LHC.

For indirect searches of BSM physics the CLIC strategy involves high precision measurements of parameters and couplings of the SM. In this way, the searches can reach sensitivities beyond the centre-of-mass energy of the collider. An example is reported in [15], where the process $e^+e^- \to \mu^+\mu^-$ is studied in the frame of the minimal anomaly-free Z' model. The 5σ discovery limit as a function of the integrated luminosity illustrates how the discovery can be extended to new particles with masses up to tens of TeV (Figure 13).

5 Summary and conclusions

CLIC is a mature international project with the aim of building an electron-positron linear collider with centre-of-mass energy spanning from a few hundred GeV up to 3 TeV. Thanks to its energy staging and the high luminosity foreseen, CLIC is a precision machine with a unique physics potential. Already in the first stage, the Higgs boson couplings and width can be measured with high precision. Moreover, a dedicated programme for the top quark is foreseen to extract its mass, width and other properties with very low uncertainties. At higher-energy stages, the programme will extend to search for rare Higgs processes and decays, as well as for BSM physics up to several tens of TeV with both direct and indirect measurements.

On the accelerator side, the technical challenges of such a high-energy linear collider are solved using a two-beam acceleration scheme, whose proof-of-concept was demonstrated. The CLIC environment and physics goals, especially in the highest energy stage, lead to strict requirements on both the detector and the software. The CLIC detector model, using cutting-edge technology and thoroughly optimised by simulation, has proven to fulfil them all.

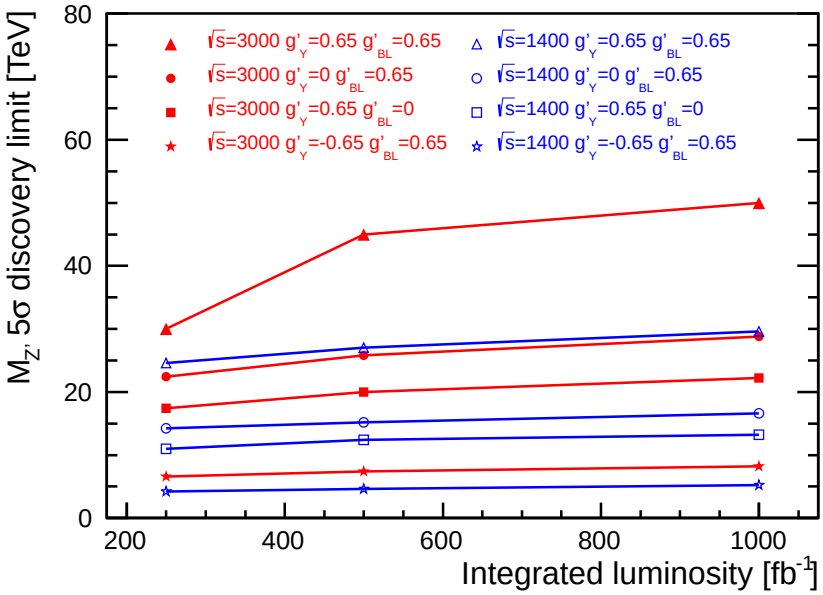

Figure 13: Z' mass discovery limit at 5σ from the measurement $e^+e^- \to \mu^+\mu^-$ as a function of the integrated luminosity and for different coupling values in the minimal anomaly-free Z' model [2].

References

[1] L. Linssen et al., eds., *CLIC Conceptual Design Report: Physics and Detectors at CLIC*, CERN-2012-003, CERN, 2012, arXiv: 1202.5940 [physics.ins-det].

[2] P. Burrows, et al (Eds), *Updated baseline for a staged Compact Linear Collider* (2016), CERN-2016-004, URL: http://dx.doi.org/10.5170/CERN-2016-004.

[3] T. Charles et al., *The Compact Linear e^+e^- Collider (CLIC) – 2018 Summary Report*, arXiv:1812.06018, 2018, URL: https://cds.cern.ch/record/2652188.

[4] P. G. Roloff, A. Robson, *Updated CLIC luminosity staging baseline and Higgs coupling prospects*, CLICdp-Note-2018-002 (2018), URL: https://cds.cern.ch/record/2645352.

[5] D. Arominski et al., *A detector for CLIC: main parameters and performance*, CLICdp-Note-2018-005 (2018), URL: https://cds.cern.ch/record/2649437.

[6] N. Alipour Tehrani et al., *CLICdet: The post-CDR CLIC detector model*, CLICdp-Note-2017-001 (2017), URL: http://cds.cern.ch/record/2254048.

[7] M. Frank et al., *DD4hep: A Detector Description Toolkit for High Energy Physics Experiments*, J. Phys. Conf. Ser. **513** (2013) 022010.

[8] S. Agostinelli et al., *Geant4-a simulation toolkit*, Nucl. Instr. Meth. Phys. A **506** (2003) 250, ISSN: 0168-9002, DOI: https://doi.org/10.1016/S0168-9002(03)01368-8, URL: http://www.sciencedirect.com/science/article/pii/S0168900203013688.

[9] M. Frank et al., *DDG4: A Simulation Framework using the DD4hep Detector Description Toolkit*, J. Phys. Conf. Ser. **664** (2015) 072017.

[10] E. Brondolin, A. Sailer, *Optimization of timing selections at 380 GeV CLIC*, tech. rep. arXiv:1811.00466, Geneva: CERN, 2018, URL: http://cds.cern.ch/record/2645355.

[11] H. Abramowicz et al., *Higgs physics at the CLIC electron-positron linear collider*, Eur. Phys. J. **C77** (2017) 475, DOI: 10.1140/epjc/s10052-017-4968-5, arXiv: 1608.07538 [hep-ex].

[12] H. Abramowicz et al., CLICdp, *Top-Quark Physics at the CLIC Electron-Positron Linear Collider* (2018), arXiv: 1807.02441 [hep-ex].

[13] W. Bernreuther et al., *CP-violating top quark couplings at future linear e^+e^- colliders*, Eur. Phys. J. **C78** (2018) 155, DOI: 10.1140/epjc/s10052-018-5625-3, arXiv: 1710.06737 [hep-ex].

[14] J. de Blas et al., *The CLIC Potential for New Physics*, tech. rep. arXiv:1812.02093, 2018, URL: https://cds.cern.ch/record/2650541.

[15] J.-J. Blaising, J. D. Wells, *Physics performances for Z' searches at 3 TeV and 1.5 TeV CLIC* (2012), arXiv: 1208.1148 [hep-ph].